Indian Journal of Chemistry
Vol. 65, April 2026, pp. 368-382
DOI: 10.56042/ijc.v65i4.28374

# Synthesis and photophysical properties of aromatic L-amino acids functionalized tricyanofuran (TCF) derivatives

Gayatri Jagdale[a], Dnyaneshwar D Ugale[a,b], Sudhir D Jagadale[a], Dinesh N Nadimetla[c], Avinash L Puyad[d], Shailaja B Jadhav[e], Sheshanath V Bhosale[f] & Sidhanath V Bhosale*[a,b]

[a] Polymers and Functional Materials Division, CSIR-Indian Institute of Chemical Technology, Tarnaka, Hyderabad 500 007, Telangana, India

[b] Academy of Scientific and Innovative Research (AcSIR), CSIR-HRDC Campus, Postal Staff College Area, Sector 19, Kamla Nehru Nagar, Ghaziabad 201 002, Uttar Pradesh, India

[c] Department of Catalysis and Fine Chemicals, CSIR-Indian Institute of Chemical Technology, Tarnaka, Hyderabad 500 007, Telangana, India

[d] School of Chemical Sciences, Swami Ramanand Teerth Marathwada University, Nanded 431 606, Maharashtra, India

[e] Department of Pharmaceutical Chemistry, P. E. S. Modern College of Pharmacy, Nigadi, Pune 411 044, Maharashtra, India

[f] Department of Chemistry, School of Chemical Sciences, Central University of Karnataka, Kadaganchi, Kalaburagi 585 367, Karnataka, India

E-mail: bhosale.iict@csir.res.in

*Received 6 February 2026; accepted (revised) 2 April 2026*

Fluorescent labelling using chemical dyes is extensively used in biological and medicinal research. The amino acid incorporated chromophores with significant fluorescence properties are commonly used as fluorescent imaging agents allowing to tap a wide range of biological and biophysical processes. The dyes with large size can disrupt protein folding and function. Therefore, the development of new fluorophores remains a challenging task for the design of new fluorescent probes. To achieve the desired applications, small fluorescent chromophores are required. Herein, inspired by the earlier reports on fluorescent fluorophore, a new class of small organic chromophores is reported, containing (*E*)-2-(4-(4-aminostyryl)-3-cyano-5,5-dimethylfuran-2(5*H*)-ylidene) malononitrile (TCF-1) that can be conjugated with the natural aromatic amino acids *i.e.* L-phenylalanine, L-tryptophan and L-tyrosine. In this connection, a series of six TCF-1 fluorescently labeled aromatic amino acids have been designed and synthesized. At first, the theoretical calculations have been performed to establish the frontier molecular orbitals and energy band gap. Further, the synthesized aromatic amino acid functionalized TCF-1 have been evaluated with respective to their spectroscopic properties using UV-Vis absorption and fluorescence spectroscopic techniques. The promising photophysical properties of Boc protected derivatives Boc-L-Phe-TCF-1, Boc-L-Tyr-TCF-1 and Boc-L-Trp-TCF-1 have been observed in different solvents. Moreover, the Boc deprotected derivatives L-Phe-TCF-1, L-Tyr-TCF-1 and L-Trp-TCF-1 show different photophysical properties at various *p*H ranging from 3 to 11.

**Keywords:** Fluorescent fluorophore, Amino acids, TCF, UV-Vis, Photophysical properties

In modern era of biological sciences, the monitoring of the genetic functions in a cell has attracted researchers' interest[1]. In this connection, the fluorescence-based method has been utilized to understand and monitor the localization, trafficking and expression of biomolecules in tissues and live cells[2]. Significant development in the fluorescent probes due to their high selectivity, sensitivity and fast response time and relative ease in manipulating the photophysical properties have revolutionized the research field[3]. It is interesting to note that, in various biological processes such as enzyme mechanism[4] and protein-protein interactions, many biological peptides and proteins play a crucial role[5]. The investigation of these processes in biosystems can be achieved by directly visualizing with fluorescent spectroscopy techniques such as resonance energy transfer (RET), namely bioluminescence-RET (BRET) and fluorescence-RET (FRET), and bimolecular fluorescence complementation (BiFC)[6]. Though the RET and BiFC assays are important techniques for the visualization and examination of the non-covalent interactions occuring in live cells and organisms but these methods displayed drawback in the cell study of protein complexes due to behavioural aspect of fusion protein compared to their native counterpart and they did not exhibit strong fluorescence emission. Therefore, to solving this problem, the protein-protein

interaction study could be achieved using fluorescent protein in combination with fluorescence spectroscopy method. The peptide and protein labeling was successfully achieved using naturally occuring green fluorescent protein (GFP) and their derivative[7] or naturally occuring fluorescent α-amino acids within a protein structure[8]. These methods have led to significant biological discoveries but they exhibited limitations related to the biomolecular properties alteration and stability of fluorescent protein as well as the functionality of their fusion partner protein. The use of fluorescent α-amino acids within a protein relies on the relative abundance of it within the protein structure and the presence of their residues also caused complicated fluorescence spectroscopic response[7,8]. To tackle the limitations such as poor photoluminescence properties displayed by naturally occuring fluorescent α-amino acids *i.e*. L-phenylalanine, L-tyrosine and L-tryptophan[9], an alternative approach such as design and development of unnatural fluorescent amino acid and their analogues[10]. The photophysical characteristics of the unnatural fluorescent α-amino acids can be manipulated for a desired application[11]. Significant developments in research fields to improve the fluorescent properties of L-phenylalanine, L-tyrosine and L-tryptophan as potential isosteric substitutes in proteins was achieved[12]. However, there is a great room for the development of unnatural fluorophore conjugated amino acids such as L-phenylalanine, L-tyrosine and L-tryptophan to minimize the disruption of protein structure and function. Such fluorescent dye development could be useful to accelerate the research in molecular and cellular biology, biophysics, biotechnology and medicine due to their high fluorescent emission properties.

The structural modification of the L-phenylalanine, L-tyrosine and L-tryptophan can be used for developing fluorescent unnatural amino acid analogues. Inspired by the work reported in the literature, we have sought to design and develop L-phenylalanine, L-tyrosine and L-tryptophan functionalized (*E*)-2-(4-(4-aminostyryl)-3-cyano-5,5-dimethylfuran-2(5*H*)-ylidene) malononitrile (TCF-1) analogues. In this regard, we now report the synthesis of series of novel TCF-1-derived amino acids and demonstrate their electronic properties using theoretical calculations. We also describe the photophysical properties of *tert*-butyl (*S*,*E*)-(1-((4-(2-(4-cyano-5-(dicyanomethylene)-2,2-dimethyl-2,5-dihydrofuran-3-yl)vinyl)phenyl) amino)-1-oxo-3-phenyl-propan-2-yl)carbamate (Boc-L-Phe-TCF-1), *tert*-butyl *(S,E)*-(1-((4-(2-(4-cyano-5-(dicyanomethylene)-2,2-dimethyl-2,5-dihydrofuran-3-yl)vinyl)phenyl)amino)-3-(4-hydroxyphenyl)-1-oxopropan-2-yl)carbamate (Boc-L-Tyr-TCF-1) and tert-butyl (S,E)-(1-((4-(2-(4-cyano-5-(dicyanomethylene)-2,2-dimethyl-2,5-dihydrofuran-3-yl)vinyl)phenyl) amino)-3-(1*H*-indol-3-yl)-1-oxopropan-2-yl) carbamate (Boc-L-Trp-TCF-1) in various solvents. Moreover, the boc deprotected derivatives such as (*S*,*E*)-2-amino-*N*-(4-(2-(4-cyano-5-(dicyano-methylene)-2,2-dimethyl-2,5-dihydro-furan-3-yl)vinyl)phenyl)-3-phenyl propanamide (L-PheTCF-1), (*S*,*E*)-2-amino-N-(4-(2-(4-cyano-5-(dicyanomethylene)- 2,2-dimethyl-2,5-dihydrofuran-3-yl)vinyl) phenyl)-3-(4-hydroxyphenyl)propanamide (L-Tyr-TCF-1) and (*S*,*E*)-2-amino-*N*-(4-(2-(4-cyano-5-(dicyano- methylene)-2,2-dimethyl-2,5-dihydrofuran-3-yl)vinyl) phenyl)-3-(1*H*-indol-3-yl)propanamide (L-Trp-TCF-1) are prepared from Boc-L-Phe-TCF-1, Boc-L-Tyr-TCF-1 and Boc-L-Trp-TCF-1, respectively. Then, the photophysical properties of as-prepared L-PheTCF-1, L-Tyr-TCF-1 and L-Trp-TCF-1 also examined at various *p*H. We presume that the present investigation could help to have a new series of fluorescent dyes to establish the molecular binding events *e.g*. protein-protein interactions in biological applications.

## Experimental Section

### Materials and methods

The chemicals, reagents and solvents were purchased from commercial sources and were utilized as received unless mentioned otherwise. The reaction progress was monitored by analytical thin layer chromatography (TLC) using Merck TLC aluminium sheets (silica gel 60 F254). Spot of product observe with UV-Vis and Fluorescence light. IR spectra were recorded on a Therma Nicolet Nexus 670 FT-IR spectrometer in the form of KBr pellets. $^{1}$H NMR spectra were measured on a Bruker Avance 400 and 500 MHz spectrometer at the ambient temperature of $^{1}$H at 400 and 500 MHz as indicated in the experimental date. $^{13}$C NMR spectra were also recorded on a Bruker Avance 400 and 500 MHz spectrometer at the ambient temperature of $^{13}$C at 101 and 126 MHz. $^{1}$H and $^{13}$C Chemical shifts are reported in ppm downfield from tetramethyl silane (TMS. δ scale) with a solvent resonance as internal

standards. Mass spectrometric data were obtained by positive electron spray ionization (ESI-MS) technique on an Agilent Technologies 1100 Series (Agilent Chem-station Software) mass spectrometer. High-resolution mass Spectrometry (HRMS) were recorded by using ESIQTOF mass spectrometry. UV-Vis absorption spectra were measured on a Shimadzu UV-1800 spectrophotometer at RT. Fluorescence emission spectra were mesured on an RF-6000 (Shimadzu, Japan) Spectro fluoro-photometer. All experiments were performed in a Quartz cell with a 1 cm path length and 370 nm excitation wavelength.

**Synthesis protocols**

**Synthesis of 2-(3-cyano-4,5,5-trimethylfuran-2(5*H*)-ylidene)malononitrile (TCF), 2** (Ref. 13)

3-Hydroxy-3-methyl-2-butanone (0.3 g, 2.9 mmol) and malononitrile (0.40 g, 6.1 mmol) were dissolved in anhydrous EtOH (10 mL). The reaction mixture was stirred at RT. Then sodium ethoxide (0.065 g, 0.9 mmol) was added and the reaction mixture was further heated at reflux for 3 h. After completion of reaction (monitored by TLC). The reaction mixture was cooled down to RT. The obtained reaction mass was filtered through a Buchner funnel. The solid residue was washed with ethanol. Then the reaction mass was directly recrystallized and using ethanol to give the corresponding product **2** as TCF (off-white crystalline solid) (yield: 66%).

$^1$H NMR (500 MHz, $CDCl_3$): δ 2.37 (s, 3H), 1.63 (s, 6.00H); $^{13}$C NMR (126 MHz, $CDCl_3$): δ 182.6, 175.2, 111.0, 110.4, 109.0,99.8, 58.9, 24.2, 14.2; FT-IR (KBr): 2998 (C-H Stretch), 2235 (C-N Nitrile), 1418 (Aromatic C=C Stretch), 1158 cm$^{-1}$ (C-O Ether); ESI-MS: *m/z* 198 $(M-H)^+$; HRMS: Calcd for $C_{11}H_9ON_3$: 200.0818. Found: 200.0815.

**Synthesis of (*E*)-2-(3-cyano-5,5-dimethyl-4-(4-nitrostyryl)furan-2(5*H*)ylidene) malononitrile, 3**

4-Nitrobenzaldehyde (1.13 g, 7.5 mmol) and TCF (**2**) (1.0 g, 5.0 mmol) were dissolved in absolute ethanol (20 mL) and stirred at RT. for 10 min. Then ammonium acetate (0.19 g, 7.5 mmol) was added to this reaction mixture. The reaction mixture was stirred at 60°C for 12 h. The completion of reaction was confirmed using TLC. Then, the reaction mixture was cooled to RT. The brown precipitate was obtained. The crude brown solid was washed with ethanol and dried under vacuum to afford compound **3** as a pale-brown powder (yield: 85%). $^1$H NMR (400 MHz, DMSO-$d_6$): δ 8.32 (d, $J$ = 8.7 Hz, 2H), 8.18 (d, $J$ = 8.7 Hz, 2H), 7.97 (d, $J$ = 16.6 Hz, 1H), 7.41 (d, $J$ = 16.6 Hz, 1H), 1.82 (s, 6H); $^{13}$C NMR (101 MHz, DMSO-$d_6$): δ 192.8, 177.2, 174.4, 149.0, 144.2, 140.8, 130.7, 124.6, 119.6, 112.9, 100.0, 55.9, 25.4; FT-IR (KBr): 3200 (C-H Stretch), 2225 (C-N Nitrile), 1568 (Aromatic C=C Stretch), 1413 (N-O), 1108 cm$^{-1}$ (C-O Ether); ESI-MS: *m/z* 332 $(M)^+$ HRMS: Calcd for $C_{18}H_{11}O_3N_4$: 331.0825. Found: 331.0840.

**Synthesis of (*E*)-2-(4-(4-aminostyryl)-3-cyano-5,5-dimethylfuran-2(5*H*)ylidene) malononitrile, 4 (TCF-1)**

A solution of compound **3** (0.3 g, 0.90 mmol) and stannous chloride, dihydrate ($SnCl_2.2H_2O$) (1.22 g, 5.4 mmol) were dissolved in ethyl acetate (20 mL). The reaction mixture was stirred at RT. for 12 h. After completion of reaction (monitored by TLC), the reaction mass was extracted with ethyl acetate. The organic layers collected was subjected for drying over $Na_2SO_4$. The solvent was removed by evaporation under reduced pressure. The extracted reaction mass residue was directly purified by column chromatography to silica gel (hexane /ethyl acetate, 2:1) to give the corresponding products TCF-1, **4** as a red powder (yield 88%).

$^1$H NMR (500 MHz, DMSO-$d_6$): δ 7.87 (d, $J$ = 15.7 Hz, 2H), 7.67 (d, $J$ = 8.4 Hz, 2H), 6.81(d, $J$ = 15.8 Hz, 2H), 6.67 (d, $J$ = 8.6 Hz, 2H), 1.74 (s, 6H); $^{13}$C NMR (101 MHz, DMSO-$d_6$): δ 192.8, 177.2, 174.4, 149.0, 144.2,140.8, 131.1, 130.7, 124.6, 119.6, 112.9, 100.0, 55.9, 25.4; FT-IR (KBr): 3438 (N-H Stretch) 3200 (C-H Stretch), 2228 (C-N Nitrile), 1557 (Aromatic C=C Stretch), 1168 cm$^{-1}$ (C- O Ether); ESI-MS: *m/z* 301 $(M-H)^+$; HRMS: Calcd for $C_{18}H_{15}ON_4$: 303.1240. Found: 303.1235.

**Synthesis of (tert-butoxycarbonyl)phenylalanine (Boc-L-Phe)**

The compound L-phenylalanine (1.00 g, 6.05 mmol) was dissolved in 15 mL of 1 N NaOH. Then the as-prepared solution of $(Boc)_2O$ (2.90 g, 13.3 mmol) in THF (10 mL) was added to the solution of L-phenylalanine. The *p*H of the reaction mixture was maintained between *p*H 9 and 11 with the addition of 1 N NaOH. The reaction mixture was stirred at RT. for 12 h. After completion of the reaction (monitored by TLC), the THF was evaporated in vacuum with the residues being adjusted to *p*H 4–5 with 1 N aq. citric acid. Then the reaction mass was extracted with ethyl acetate (3×25 mL). The obtained ethyl acetate extracts were combined,

washed with brine (3×20 mL) and then dried over $MgSO_4$. The evaporation of organic yields crude product, which was directly purified by column chromatography on silica gel to give the corresponding product Boc-L-Phe as oily white solid (yield: 77.5%). $^1$H NMR (400 MHz, $CDCl_3$): δ 9.01 (s, 1H), 7.23 (s, 1H), 7.22 (s, 1H), 7.20 (s, 1H), 7.18 (s, 1H), 7.17 (s, 1H), 7.11 (s, 1H), 4.96 (s, 1H), 3.12 (d, *J* = 8.0 Hz, 2H), 1.34 (s, 9H); $^{13}$C NMR (101 MHz, DMSO-$d_6$): δ 171.6, 150.6, 131.7, 131.1, 124.6, 123.8, 75.5, 49.7, 33.1, 23. 5; FT-IR (KBr): 3441 (N-H Stretch) 3441 (O-H Stretch), 2983 (C-H Stretch), 1640 (C=O-OR Ester), 1567 (C=O-NH Stretch), 1418 cm$^{-1}$ (Aromatic C=C Stretch); ESI-MS: *m/z* 303 $(M-H)^+$; HRMS: Calcd for $C_{14}H_{18}O_4N$: 264.1241. Found: 264.1241.

**Synthesis of (*tert*-butoxy carbonyl) tyrosine (Boc-L-Tyr)**

The product Boc-L-Tyr as sticky white solid (Yield: 66%) was obtained following the procedure for the preparation of Boc-L-Phe given in section 2.2.4 after column chromatography on silica gel. $^1$H NMR (500 MHz, $CDCl_3$): δ 7.10 (s, 1H), 7.09 (s, 1H), 7.01 (d, *J* = 8.5 Hz, 1H), 6.89 (d, *J* = 8.1 Hz, 1H), 6.63 (d, *J* = 7.9 Hz, 1H), 4.48 (t, *J* =14.7 Hz, 1H), 2.90 (d, *J* = 39.4 Hz, 2H), 1.33 (s, 9H); $^{13}$C NMR (101 MHz, $CDCl_3$): δ 175.9, 155.0, 130.5, 121.3, 115.6, 80.7, 54.5, 37.0, 28.3; FT-IR (KBr): 3415 (N-H Stretch) 3415 (O-H Stretch) 2983 (C-H Stretch), 2236 (C-N Nitrile), 1677 (C=O-OR Ester), 1642 (C=O-NH Stretch) 1571 cm$^{-1}$ (Aromatic C=C Stretch); ESI-MS: *m/z* 280 $(M-H)^+$; HRMS: Calcd for $C_{14}H_{18}O_5N$: 280.1179. Found: 280.1189.

**Synthesis of (*tert*-butoxycarbonyl)tryptophan (Boc-L-Trp)**

The product Boc-L-Trp as white soild (Yield: 65%) was obtained following the procedure for the preparation of Boc-L-Phe given in section 2.2.4 after column chromatography on silica gel (Yield: 65%). $^1$H NMR (400 MHz, DMSO-$d_6$): δ 12.52 (s, 1H), 10.83 (s, 1H), 7.51 (s, 1H), 7.33 (s, 1H), 7.14 (s, 1H), 7.07 (s, 1H), 6.98 (s, 2H), 4.15 (s, 1H), 3.12 (s, 1H), 2.98 (s, 1H), 1.33 (s, 9H); $^{13}$C NMR (101 MHz, DMSO-$d_6$): δ 174.2, 155.8, 155.5, 136.5, 127.2, 124.1, 121.5, 118.6, 111.9, 110.4, 78.6, 55.0, 28.6, 27.3; FT-IR (KBr): 3406 (N-H Stretch) 3406 (O-H Stretch) 2980 (C-H Stretch), 1675 (C=O-OR Ester), 1574 (C=O-NH Stretch), 1414 cm$^{-1}$ (Aromatic C=C Stretch); ESI-MS: *m/z* 303 $(M-H)^+$; HRMS: Calcd for $C_{16}H_{21}O_4N_2$: 305.1495. Found: 305.1492.

**Synthesis of *tert*-butyl (*E*)-(1-((4-(2-(4-cyano-5-(dicyanomethylene)-2,2-dimethyl-2,5-dihydrofuran-3-yl) vinyl)phenyl)amino)-1-oxo-3-phenylpropan-2-yl)carbamate (Boc-L-Phe-TCF-1)**

Compound Boc-L-Phe (0.394 g, 1.48 mmol) and HATU (0.377 g, 0.99 mmol) were dissolved in DMF (15 mL). The reaction mixture was stirred under nitrogen atmosphere at 0°C for 30 min. Then DIPEA (0.213 g, 1.65 mmol) was added to the above reaction mixture. The reaction mixture was further stirred for 15 min. To this reaction mixture TCF-1 (**4**) (0.3 g, 0.99 mmol). was added subsequently. Then the reaction was continued for further 48 h with constant stirring. The progress of the reaction was examined by the thin layer chromatography (TLC). After consumption of reaction, the reaction mixtures poured into ice water and allow to stirred for 30 min. Then filter out this reaction mixture and directly purified by column chromatography using silica gel to yield Boc-L-Phe-TCF-1 as a purple color solid (0.38 g, 69.5%). $^1$H NMR (400 MHz, DMSO-$d_6$): δ 10.45 (s, 1H), 7.89 (t, *J* = 11.3 Hz, 2H), 7.75 (d, *J* = 8.7 Hz, 1H), 7.68 (d, *J* = 8.6 Hz, 1H), 7.30 (s, 2H), 7.27 (d, *J* = 8.0 Hz, 2H), 7.21 (s, 1H), 7.14 (d, *J* = 16.5 Hz, 1H), 6.82 (d, *J* = 15.8 Hz, 1H), 6.66 (d, *J*= 8.6 Hz, 1H), 4.35 (s, 1H), 3.02 (s, 1H), 2.88 (s, 1H), 1.74 (s, 9H),1.32 (s, 6H); $^{13}$C NMR (126 MHz, $CDCl_3$): δ 204.0, 182.0, 177.0, 160.4, 154.8, 136.0, 134.4, 133.4, 131.4, 130.5, 126.9, 124.5, 119.6, 112.8, 103.3, 96.7, 83.4, 58.8, 47.0, 33.3, 31.6, 23.3, 21.3; FT-IR (KBr): 3300 (N-H Stretch), 3300(O-H Stretch),2985 (C-H Stretch), 2230 (C-N Nitrile), 1638 (C=O- OR Ester), 1563 (C=O-NH Stretch),1418 (Aromatic C=C Stretch), 1173 cm$^{-1}$ (C-O Ether); ESI-MS: *m/z* 548 $(M-H)^+$; HRMS: Calcd for $C_{32}$ $H_{30}$ $O_4$ $N_5$: 548.2292. Found: 548.2301.

**Synthesis of *tert*-butyl*(S,E)*-(1-((4-(2-(4-cyano-5-(dicyanomethylene)-2,2-dimethyl-2,5-dihydrofuran-3-yl)vinyl)phenyl)amino)-3-(4-hydroxyphenyl)-1-oxopropan-2-yl)carbamate (Boc-L-Tyr-TCF-1)**

The product Boc-L-Tyr-TCF-1was obtained following the procedure for the preparation of Boc-L-Phe-TCF-1 after column chromatography as a purple color solid (0.35 g, 62.5%). $^1$H NMR (400 MHz, DMSO-$d_6$): δ 7.88 (d, *J* = 15.8 Hz, 2H), 7.67 (d, *J* = 8.7 Hz, 2H), 7.35 (s, 1H), 7.10 (d, *J* = 8.3 Hz, 2H), 6.85 (d, *J* = 9.1 Hz, 2H), 6.67 (d, *J* = 8.8 Hz, 2H), 4.38 (s, 1H), 3.13 – 2.95 (m, 2H), 1.74 (s, 9H), 1.37 (s, 6H); $^{13}$C NMR (101 MHz, DMSO-$d_6$): δ 177.7, 176.0, 156.5, 155.6, 150.6, 140.7, 134.1, 131.7, 130.8, 130.6, 122.1, 121.4, 114.7, 114.0, 113.2, 98.2, 91.8,

78.9, 53.4, 51.1, 28.6, 27.7, 25.9; FT-IR (KBr): 3461 (N-H Stretch) 3461 (O-H Stretch) 2985 (C-H Stretch), 2225 (C-N Nitrile), 1634 (C=O-OR Ester), 1609 (C-O Ether),1573 (C=O-NH Stretch), 1415 $cm^{-1}$ (Aromatic C=C Stretch); ESI-MS: *m/z* 564 $(M-H)^+$; HRMS: Calcd for $C_{32}H_{30}O_5N_5$: 564.2252. Found: 564.2250.

**Synthesis of *tert*-butyl (*E*)-(1-((4-(2-(4-cyano-5-(dicyanomethylene)-2,2-dimethyl-2,5-dihydrofuran-3-yl)vinyl)phenyl)amino)-3-(1*H*-indol-3-yl)-1-oxo-propan-2-yl)carbamate (Boc-L-Trp-TCF-1)**

The product Boc-L-Trp-TCF-1 as a purple color solid (0.38 g, 65.5%) was obtained following the procedure for the preparation of Boc-L-Phe-TCF-1 after column chromatography. $^1$H NMR (400 MHz, DMSO-$d_6$): δ 10.84 (s, 1H), 10.00 (s, 1H), 8.22 (s, 1H), 7.88 (d, *J* = 15.7 Hz, 1H), 7.68 (d, *J* = 8.6 Hz, 1H), 7.52 (dd, *J* = 27.8, 9.9 Hz, 1H), 7.31 (s, 1H), 7.16 (s, 1H), 7.06 (s, 1H), 6.98 (s, 1H), 6.89 – 6.79 (m,1H), 6.66 (d, *J* = 8.6 Hz, 1H), 6.66 (d, *J* = 8.6 Hz, 1H), 3.55 (s, 1H), 3.07 (d, *J* = 19.1 Hz, 2H), 1.33 (s, 6H), 1.21 (s, 9H); $^{13}$C NMR (101MHz, $CDCl_3$): δ 198.0, 181.3, 160.7, 155.0, 141.2, 138.9,132.6, 132.3, 128.9, 127.2, 126.3, 124.2, 123.4, 119.4,118.8, 117.3, 112.9, 103.6, 99.7, 96.7, 94.7, 61.4, 58.7, 33.4, 30.9, 23.4, 21.1; FT-IR (KBr): 3473 (N-H Stretch) 3473 (O-H Stretch),2981 (C-H Stretch), 2175 (C-N Nitrile), 1669 (C-O Ether), 1650 (C=O-OR Ester), 1570 (C=O-NH Stretch), 1418 $cm^{-1}$ (Aromatic C=C Stretch); ESI-MS: *m/z* 587 $(M-H)^+$; HRMS: Calcd for $C_{34}H_{31}O_4N_6$: 587.2401. Found: 587.2408.

**Synthesis of (*E*)-2-amino-N-(4-(2-(4-cyano-5-(dicyanomethylene)-2,2-dimethyl-2,5-dihydrofuran-3-yl)vinyl)phenyl)-3-phenylpropanamide (L-Phe-TCF-1)**

Trifluoroacetic acid (5 mL) was added drop-wise to a stirred suspension of Boc-L-Phe-TCF-1 (0.3 g, 0.5 mmol) in DCM (10 mL) at 0°C. The resulting solution was stirred at RT. for 6 h. The solvent was removed under reduced pressure using rotary evaporator. The residue was treated with n-hexane (3×50 mL) to remove excess of TFA under reduced pressure to afford a desired product L-Phe-TCF-1 as a white solid (0.13 g,58%). $^1$H NMR (300 MHz, DMSO-$d_6$): δ 10.77 (s, 1H), 8.35 (s, 1H), 8.26 (s, 1H), 8.02 – 7.93 (m, 1H), 7.92 (d, *J* = 3.5 Hz, 1H),7.87 (d, *J* = 4.7 Hz, 1H), 7.69 (d, *J* = 2.4 Hz, 1H), 7.66 (d, *J* = 2.3 Hz, 1H), 7.39 – 7.30 (m, 1H), 7.29 (d, *J* = 4.1 Hz, 1H), 7.16 (d, *J* =16.5 Hz, 1H), 6.75 (dd, *J* = 46.2, 12.2 Hz, 1H), 4.10 (d, *J* = 46.6 Hz, 1H), 3.14 (d, *J* = 17.2 Hz, 2H), 1.24 (s, 6H); $^{13}$C NMR (101 MHz, DMSO-$d_6$): δ 196.0, 172.4, 162.2, 141.9, 135.3, 134.4, 130.2,129.3, 129.0, 127.8, 122.7, 120.1, 114.7, 113.2, 112.5, 108.1, 99.7, 91.9, 54.2, 42.3, 37.5, 25.6; FT-IR (KBr): 3458 (N-H Stretch) 3458 (O-H Stretch), 2988 (C-H Stretch), 2227 (C-N Nitrile), 1642 (C=O-OR Ester), 1567 (C=O-NH Stretch), 1418 (Aromatic C=C Stretch), 1178 $cm^{-1}$ (C-O Ether); ESI-MS: *m/z* 450 $(M+H)^+$; HRMS: Calcd For $C_{27}H_{24}O_2N_5$: 450.1924. Found: 450.1924.

**Synthesis of (*S*,*E*)-2-amino-N-(4-(2-(4-cyano-5-(dicyanomethylene)-2,2-dimethyl-2,5-dihydrofuran-3-yl)vinyl)phenyl)-3-(4-hydroxyphenyl) propanamide (L-Tyr-TCF-1)**

Trifluoroacetic acid (5 mL) was added drop-wise to a stirred suspension of compound Boc-L-Tyr-TCF-1 (0.2 g, 0.3 mmol) in DCM (10 mL) at 0°C. The resulting solution was stirred for 6h at rt. The solvent was removed under reduced pressure using rotary evaporator. The residue was treated with n-hexane (3×50 mL) to remove excess of TFA under reduced pressure to afford a white solid of compound L-Tyr-TCF-1 (1.34 g, 96%). (39) $^1$H NMR (400 MHz, DMSO-$d_6$): δ 11.54 (s, 1H),9.41 (s, 1H), 7.91 (s, 1H), 7.87 (s, 1H), 7.69 (s, 1H), 7.67 (s, 1H),6.84 (s, 1H), 6.80 (s, 1H), 6.68 (s, 2H), 6.66 (s, 2H), 4.06 (s, 1H),3.07 (d, 2H), 1.74 (s, 6H); $^{13}$C NMR (101 MHz, DMSO-$d_6$): δ 175.9, 170.9, 159.1, 156.0, 150.5, 134.0, 131.2, 122.4,114.7, 113.2, 112.9, 108.3, 99.2, 54.2, 51.5, 42.4, 36.0, 26.1; FT-IR (KBr): 3509 (N-H Stretch) 3509 (O-H Stretch),2998 (C-H Stretch), 2224 (C-N Nitrile), 1646 (C=O-OR Ester), 1571 (C=O-NH Stretch), 1418 (Aromatic C=C Stretch), 1168 $cm^{-1}$ (C-O Ether); ESI-MS: *m/z* 466 $(M+H)^+$; HRMS: Calcd for $C_{27}H_{22}O_3N_5$: 464.1717. Found: 464.1727.

**Synthesis of (*E*)-2-amino-N-(4-(2-(4-cyano-5-(dicyanomethylene)-2,2-dimethyl-2,5-dihydrofuran-3-yl)vinyl)phenyl)-3-(1*H*-indol-3-yl)propenamide (L-Trp-TCF-1)**

The product L-Trp-TCF-1 as a white solid (0.11 g, 76.5%) was obtained following the procedure for the preparation of compound L-Tyr-TCF-1 described in subsection 2.2.10.

$^1$H NMR (400 MHz, DMSO-$d_6$): δ 11.12 (s, 1H),10.52 (s, 1H), 8.51 (s, 1H), 8.37 (s, 1H), 8.32 (s, 1H), 8.06 – 7.89 (m, 1H), 7.84 – 7.65 (m, 1H), 7.54 (d, *J* = 17.7 Hz, 1H), 7.42 (d, *J* = 7.5 Hz, 1H), 7.29 (s, 1H), 7.18 – 7.08 (m, 1H), 7.02 (d, *J* = 6.9 Hz, 1H), 6.88 (d, *J* = 15.9 Hz, 1H), 6.72 (d, *J* = 8.1 Hz,

1H), 4.26 (d, $J$ = 19.2 Hz, 1H), 3.38 (d, $J$ = 21.4 Hz, 2H), 1.32 (s, 6H); $^{13}$C NMR (126 MHz, DMSO-$d_6$): δ 196.8, 174.7, 158.6, 150.7, 136.7, 134.1, 131.4, 127.6, 122.8, 121.6, 118.9, 114.8, 112.4, 107.1, 99.7, 98.8, 54.2, 42.2, 26.3, 18.5, 12.8; FT-IR (KBr): 3471 (N-H Stretch) 3471 (O-H Stretch), 2988 (C-H Stretch), 2226 (C-N Nitrile), 1669 (C=O-OR Ester), 1567 (C=O-NH Stretch), 1418 (Aromatic C=C Stretch), 1174 cm$^{-1}$ (C-O Ether); ESI-MS: *m/z* 489 $(M+H)^+$; HRMS: Calcd for $C_{29}H_{25}O_2N_6$: 489.2033. Found: 489.2025.

## Results and Discussion

The synthesis of target molecules was achieved *via* multistep organic reaction strategy. At first 2-(3-cyano-4,5,5-trimethylfuran-2(5*H*)-ylidene)malononitrile (TCF) was prepared *via* condensation reaction between 3-hydroxy-3-methyl-2-butanone and malononitrile using sodium ethoxide as catalyst by following literature reported protocol (Scheme 1a)[13]. The obtained TCF was further treated with *p*-nitobenzaldehyde in the presence of ammonium acetate to yield (*E*)-2-(3-cyano-5,5-dimethyl-4-(4-nitrostyryl)furan-2(5*H*)ylidene) malononitrile (**3**). The obtained compound **3** was treated with stannous chloride, dihydrate ($SnCl_2.2H_2O$) resulted into formation of (*E*)-2-(4-(4-aminostyryl)-3-cyano-5,5-dimethylfuran-2(5*H*) ylidene) malononitrile as TCF-1 (**4**) (Scheme 1a) with 88% yield. The TCF-1 compound was further reacted with Boc-L-Phe, Boc-L-Tyr and Boc-L-Trp *via* amide bond formation reaction using HATU and DIPEA in DMF under nitrogen atmosphere to form chromophores Boc-L-Phe-TCF-1, Boc-L-Tyr-TCF-1 and Boc-L-Trp-TCF-1, respectively (Scheme 1b). Furthermore, Boc-L-Phe-TCF-1, Boc-L-Tyr-TCF-1 and Boc-L-Trp-TCF-1 chromophores were subjected for boc deprotection reaction in the presence of TFA in dichloromethane to yield the corresponding products as L-Phe-TCF-1, L-Tyr-TCF-1 and L-Trp-TCF-1, respectively (Scheme 1b). The structure of intermediates and chromophores were characterized using $^1$H NMR, $^{13}$C NMR, FT-IR spectroscopy and mass and high resolution mass spectrometry techniques. The Boc-L-Phe-TCF-1, Boc-L-Tyr-TCF-1 and Boc-L-Trp-TCF-1 chromophores were found with high solubility in non-polar as well as polar solvents. The L-Phe-TCF-1, L-Tyr-TCF-1 and L-Trp-TCF-1 fluorophores were soluble in aqueous media.

The examination of relationship between molecular geometry and electronic characteristics of any organic molecule could be predicted most accurately using theoretical approach such as density functional theory (DFT) and time-dependent (TD)-DFT methods[14]. The

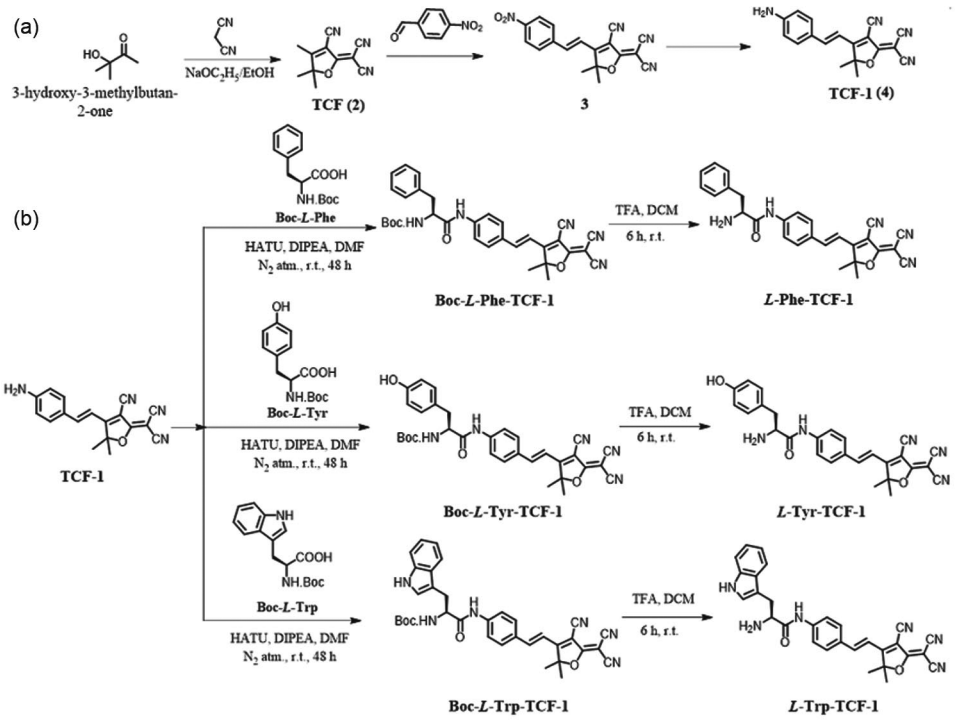


Scheme 1 — Synthetic route for (a) TCF-1 and (b) L-Phe-TCF-1, L-Tyr-TCF-1 and L-Trp-TCF-1

theoretical calculations are implemented using the Gaussian 09 *ab initio*/DFT quantum chemical simulation package to investigate the molecular geometry and frontier molecular orbitals[15]. The molecular geometries of the designed seven molecules *i.e*. TCF-1, Boc-L-Phe-TCF-1, Boc-L-Tyr-TCF-1, Boc-L-Trp-TCF-1, L-Phe-TCF-1, L-Tyr-TCF-1 and L-Trp-TCF-1 were initially optimized using B3LYP/6-31g(d) level to ensure the reliable results of the optoelectronic characteristics. Fig. 1 showed the optimized structures of the newly designed TCF, Boc-L-Phe-TCF-1, Boc-L-Tyr-TCF-1, Boc-L-Try-TCF-1, L-Phe-TCF-1, L-Tyr-TCF-1 and L-Trp-TCF-1 molecular structures, confirming the attainment of the stable geometric equilibration for the theoretical calculations. To establish the minima, frequency calculations were carried out, and all frequencies were observed to be positive, which confirms that optimized geometries are minima on the potential energy surface (PES).

The frontier molecular orbitals [FMO] such as highest occupied molecular orbitals (HOMOs) and lowest unoccupied molecular orbitals (LUMOs) of TCF, Boc-L-Phe-TCF-1, Boc-L-Tyr-TCF-1 and Boc-L-Trp-TCF-1 are shown in Fig. 2a, Fig. 2b, Fig. 2c and Fig. 2d, respectively. As shown in Fig. 2a, the HOMO and LUMO energy levels are delocalized over entire TCF-1 molecule. The estimated HOMO/LUMO energy levels of TCF-1 was -7.095/-2.070 eV. The calculated energy gap was found to be 5.025 eV. The HOMO and LUMO energy level delocalization over Boc-L-Phe-TCF-1 is shown in Fig. 2b. As

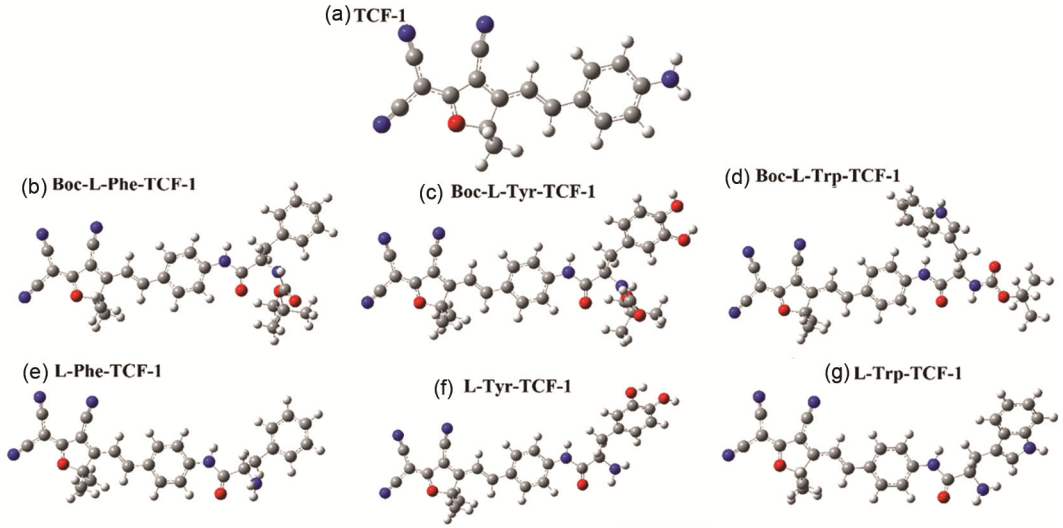


Fig. 1 — Optimized molecular structures of (a) TCF, (b) Boc-L-Phe-TCF-1, (c) Boc-L-Tyr-TCF-1 and (d) Boc-L-Try-TCF-1, (e) L-Phe-TCF-1 (f) L-Tyr-TCF-1 and (g) L-Trp-TCF-1

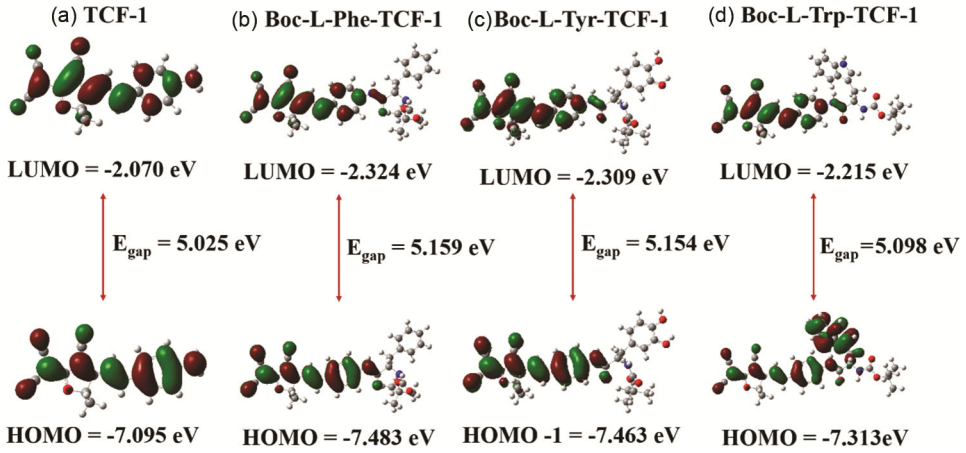


Fig. 2 — Frontier molecular orbital of (a) TCF-1, (b) Boc-L-Phe-TCF-1, (c) Boc-L-Tyr-TCF-1 and (d) Boc-L-Trp-TCF-1

demonstrated in Fig. 2b, the HOMO and LUMO energy level localized over the entire molecular backbone except the phenyl and amine subunits. The estimated energy gap from HOMO (-7.483 eV) and LUMO (-2.324 eV) was observed to be 5.159 eV. As illustrated in Fig. 2c, the HOMO and LUMO energy levels are delocalized over the Boc-L-Tyr-TCF-1 except the hydroxyphenyl and amino subunits present in the structure. The calculated energy gap using HOMO (-7.463 eV) and LUMO (-2.309 eV) energy levels was found to be 5.54 eV. As displayed in Fig. 2d, the HOMO energy level us delocalized over the entire Boc-L-Trp-TCF-1 molecular backbone except amine functional group, whereas, LUMO energy level is localized over the Boc-L-Trp-TCF-1 except the indole ring system and amine subunit. The estimated energy gap from the HOMO (-7.313 eV) and LUMO (-2.215 eV0 energy levels was observed to be 5.098 eV. These theoretical calculated results of TCF, Boc-L-Phe-TCF-1, Boc-L-Tyr-TCF-1 and Boc-L-Trp-TCF-1 indicate that on a molecular level the distribution of frontier molecular orbitals and energy levels have little influence on the structures (Fig. 2a, Fig. 2b, Fig. 2c and Fig. 2d).

FMO analysis of L-Phe-TCF-1, L-Tyr-TCF-1 and L-Trp-TCF-1 were performed for examining the electronic characteristics, chemical stability and energy band gap of organic molecules. As shown in Fig. 3a, the HOMO and LUMO energy levels are distributed over the complete molecular backbone if L-Phe-TCF-1 except the phenyl ring system and amine functional group. The FMO energy gap of the L-Phe-TCF-1 was calculated using formula $E_{gap} = E_{LUMO}$ (-2.312 eV) – $E_{HOMO}$ (-7.468 eV) and found to be 5.156 eV. The HOMO energy level is localized over entire L-Tyr-TCF-1 molecular architecture, whereas the LUMO energy level is distributed over backbone of L-Tyr-TCF-1 except hydroxyphenyl and amine subunits (Fig. 3b). The estimated molecular orbital energy gaps (ΔE) of the L-Tyr-TCF-1 was 5.117 eV determined from HOMO (-7.371 eV) and LUMO (-2.254 eV). In case of L-Trp-TCF-1, the HOMO and LUMO energy levels are distributed over the molecular backbone except indole ring system and amine functional group (Fig. 3c). The calculated HOMO and LUMO values of the L-Trp-TCF-1 are -7.74 eV and -2.241 eV, respectively, with band gap of 5.133 eV. It is important to note that, the calculated HOMO and LUMO energy values and energy band gaps of all L-Phe-TCF-1, L-Tyr-TCF-1 and L-Trp-TCF-1 does not show significant changes (Fig. 3a, Fig. 3b and Fig. 3c). Furthermore, the optimized geometries of TCF-1, Boc-L-Phe-TCF-1, Boc-L-Tyr-TCF-1, Boc-L-Trp-TCF-1, L-Phe-TCF-1, L-Tyr-TCF-1 and L-Trp-TCF-1 are considered for the time-dependent density functional theory (TD-DFT) studies using Cam-B3LYP/6-31g(d) level of theory. The Gauss-Sum program[16] was employed to analyse the TD-DFT results of seven molecules. The absorption spectras are depicted in Supplementary Information [SI†] as Figure S56 to Figure S62). From 5 the TD-DFT calculation results, the absorption peaks for TCF-1, Boc-L-Phe-TCF-1, Boc-L-Tyr-TCF-1, Boc-L-Trp-TCF-1, L-Phe-TCF-1, L-Tyr-TCF-1 and L-Trp-TCF-1 are observed at 395.22 nm (Figure S56), 386.68 nm (Figure S57), 387.33 nm (Figure S58), 390.96 nm (Figure S59), 386.61 nm (Figure S60), 388.36 nm (Figure S61) and 389.12 nm (Figure S62), respectively.

The UV–Vis absorption spectra for compounds Boc-L-Phe-TCF-1 (Fig. 4a), Boc-L-Tyr-TCF-1 (Fig. 4b) and Boc-L-Trp-TCF-1 ($1\times10^{-5}$ M) in

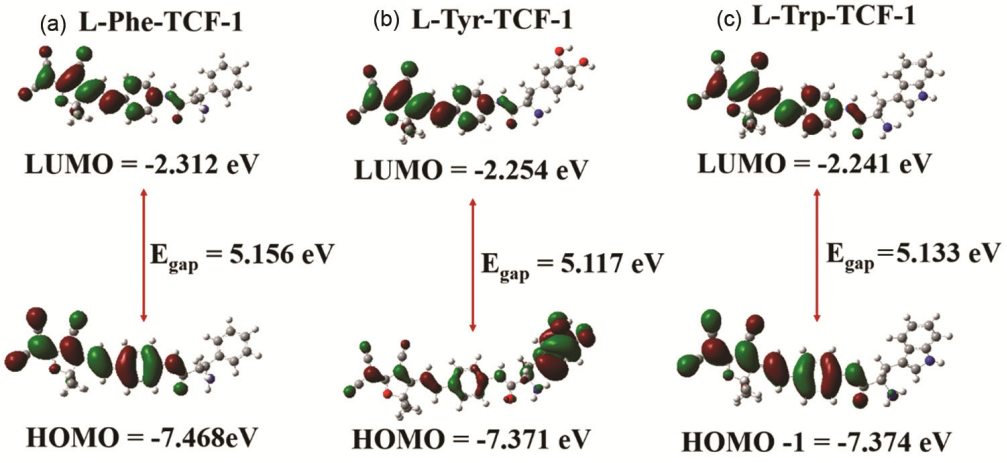


Fig. 3 — Frontier molecular orbitals of L-Phe-TCF-1, L-Tyr-TCF-1 and L-Trp-TCF-1

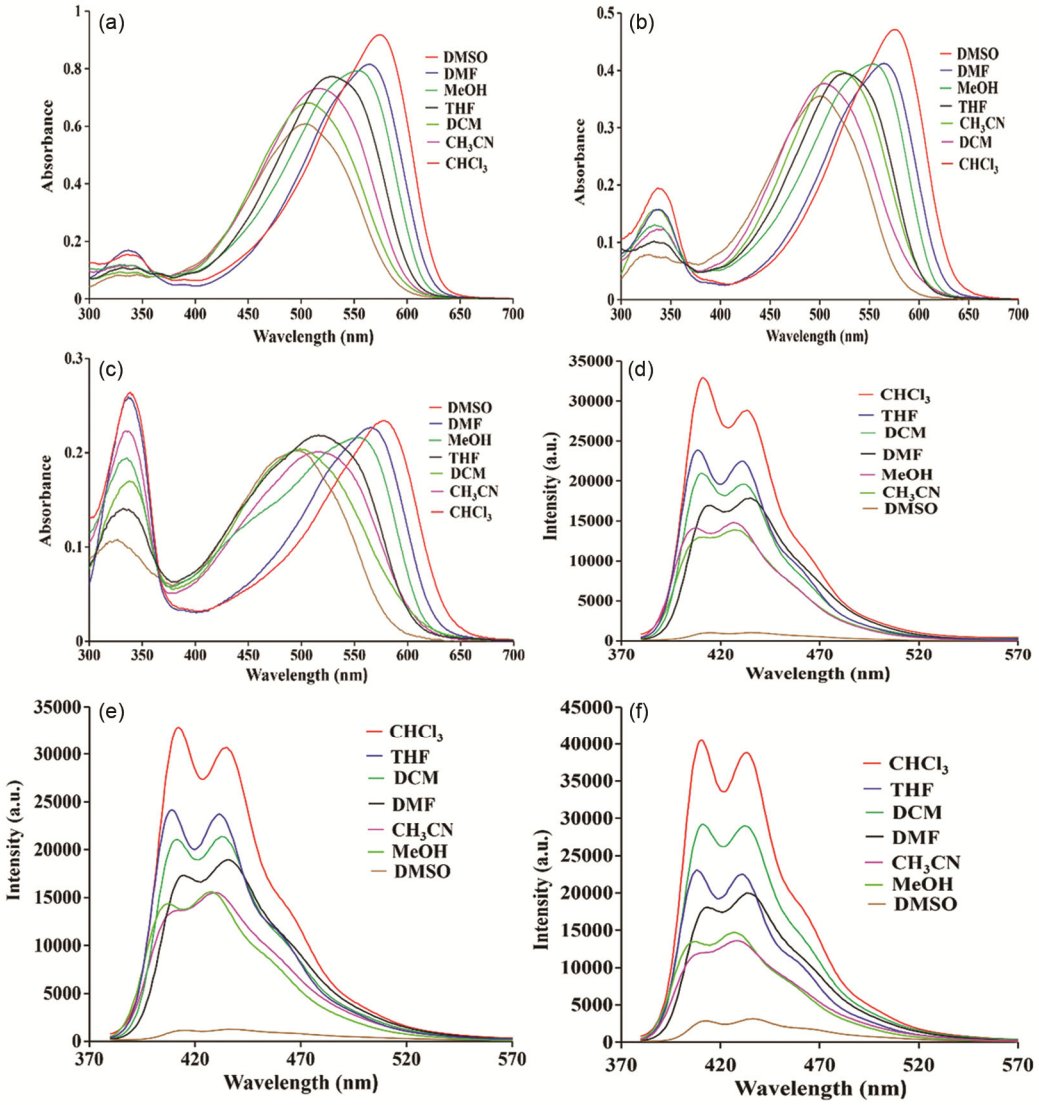


Fig. 4 — UV-Vis spectra of (a) Boc-L-Phe-TCF-1, (b) Boc-L-Tyr-TCF-1 and (c) Boc-L-Trp-TCF-1 and fluorescence spectra upon excitation at $\lambda_{ex}$ = 370 nm of (d) Boc-L-Phe-TCF-1, (e) Boc-L-Tyr-TCF-1 and (f) Boc-L-Trp-TCF-1

different solvents such as chloroform ($CHCl_3$), dichloromethane (DCM), acetonitrile ($CH_3CN$), tetrahydrofuran (THF), methanol (MeOH), dimethylformamide (DMF) and dimethylsulfoxide (DMSO) were examined at RT in the spectral region 200 to 800 nm (Fig. 4c). The absorption data is summarized in Table 1. As seen in Fig. 4a, the UV-Vis spectra of the Boc-L-Phe-TCF-1 in $CHCl_3$ displayed the characteristic absorption peak of phenylalanine with low-intensity broad band at 329 nm ($\varepsilon = 0.82\times10^4\ M^{-1}\ cm^{-1}$) and intense absorption band at 504 nm ($\varepsilon = 6.08 \times 10^4\ M^{-1}\ cm^{-1}$) for the conjugated 2-(3-cyano-4,5,5-trimethylfuran-2(5*H*)-ylidene) malononitrile (TCF-1) moiety. The absorption peaks at 329 nm and 504 nm corresponds to π-π*, n–π* and n to σ* electronic transitions, respectively. As we move from less-polar to strong polar solvents from $CHCl_3$ to DCM to $CH_3CN$ to THF to MeOH to DMF and DMSO the absorption peak position changes from 329/504 nm to 331/509 nm to 334/518 nm to 332/529 nm to 333/556 nm to 338/565 nm to 340/576 nm, respectively (Table 1). It was observed that the n to σ* electronic transition peak position displayed bathochromic shifts of about 72 nm was observed (Fig. 4a, Table 1), when we move from less polar $CHCl_3$ to strongly polar DMSO solvents. The bathochromic effect suggests the Boc-L-Phe-TCF-1 in DMSO is absorbing light at longer

Table 1 — UV-Vis absorption and fluorescence emission spectra of Boc-L-Phe-TCF-1, Boc-L-Tyr-TCF-1 and Boc-L-Trp-TCF-1 in various solvents

| Spectroscopic Methods | Solvents | Boc-L-Phe-TCF-1 | | Boc-L-Tyr-TCF-1 | | Boc-L-Trp-TCF-1 | |
|---|---|---|---|---|---|---|---|
| UV-Vis absorption spectra (nm) (Extinction coefficient ε ($M^{-1}$ $cm^{-1}$) | $CHCl_3$ | 329 (8200) | 504 (60800) | 326 (7800) | 496 (35300) | 326 (10700) | 497 (20200) |
| | DCM | 331 (9300) | 509 (68000) | 337 (12200) | 503 (37700) | 339 (16900) | 500 (20300) |
| | $CH_3CN$ | 334 (11400) | 518 (73100) | 337 (15600) | 518 (39900) | 336 (22200) | 516 (20100) |
| | THF | 332 (10800) | 529 (77200) | 335 (10000) | 526 (39500) | 333 (14000) | 518 (21800) |
| | MeOH | 333 (11800) | 556 (79200) | 335 (12900) | 554 (41100) | 337 (19200) | 557 (21500) |
| | DMF | 338 (16700) | 565 (81600) | 337 (15700) | 556 (41100) | 338 (25700) | 567 (22600) |
| | DMSO | 340 (15200) | 576 (91700) | 339 (19300) | 576 (47100) | 340 (26100) | 580 (23300) |
| Fluorescence Emisison Spectra (nm) Excitation wavelength ($\lambda_{ex}$ = 370 nm) | $CHCl_3$ | 412, 434 | | 413, 435 | | 412, 436 | |
| | DCM | 410, 432 | | 412, 434 | | 412, 433 | |
| | $CH_3CN$ | 409, 428 | | 409, 430 | | 410, 430 | |
| | THF | 409, 431 | | 410, 432 | | 410, 432 | |
| | MeOH | 407, 427 | | 408, 428 | | 407, 429 | |
| | DMF | 414, 435 | | 414, 437 | | 414, 436 | |
| | DMSO | 414, 439 (less intense peaks) | | 414, 437 (less intense peaks) | | 414, 436 (less intense peaks) | |

wavelength[17]. These UV-Vis absorption result indicates; in strongly polar solvents the effect was found to be more pronounced due to the alteration of charge density of the solute caused by the solvent, which changes the electronic distribution of Boc-L-Phe-TCF-1 and results in the solvatochromic shifts[18,19]. Moreover, the electronic environment alteration of the Boc-L-Phe-TCF-1 in strongly polar solvent DMSO resulting into a lower energy gap between the ground and excited electronic states[20]. The similar trend of the absorption changes was found for the Boc-L-Tyr-TCF-1 (Fig. 4b, Table 1) and Boc-L-Trp-TCF-1 (Fig. 4c, Table 1) in $CHCl_3$ to DCM to $CH_3CN$ to THF to MeOH to DMF and DMSO solvents. The Boc-L-Tyr-TCF-1 shows the bathochromic shift of about 80 nm on going from $CHCl_3$ (496 nm, $\varepsilon = 3.53 \times 10^4$ $M^{-1}$ $cm^{-1}$) to DMSO (576 nm, $\varepsilon = 4.76 \times 10^4$ $M^{-1}$ $cm^{-1}$) (Fig. 4b, Table 1). Similarly, Boc-L-Trp-TCF-1 (Fig. 4c, Table 1) exhibited bathochromic shifts of about 83 nm as the polarity of solvent increases from $CHCl_3$ (497 nm, $\varepsilon = 2.02 \times 10^4$ $M^{-1}$ $cm^{-1}$) to DMSO (580 nm, $\varepsilon = 2.33 \times 10^4$ $M^{-1}$ $cm^{-1}$) (Fig. 4c, Table 1). Though the π-bridge and electron acceptor subunit TCF-1 are the same in all three Boc-L-Phe-TCF-1, Boc-L-Tyr-TCF-1 and Boc-L-Trp-TCF-1 (Scheme 1b), the estimated bathochromic shifts *i.e.* 72, 80 and 83 nm, respectively, implies to a stronger intramolecular charge transfer in Boc-L-Trp-TCF-1 (Fig. 4c) than Boc-L-Tyr-TCF-1 (Fig. 4b) and Boc-L-Phe-TCF-1 (Fig. 4a).

The fluorescence emisison spectra of Boc-L-Phe-TCF-1, Boc-L-Tyr-TCF-1 and Boc-L-Trp-TCF-1 fluorophores in various solvents are shown in Fig. 4d, Fig. 4e and Fig. 4f, respectively, and their maximum emission wavelength are given in Table 1. Fig. 4d shows that Boc-L-Phe-TCF-1 exhibit a structured fluorescence emission spectrum in less polar $CHCl_3$ solvent with two intense peaks at 412 nm and 434 nm.

The emission of Boc-L-Phe-TCF-1 in $CHCl_3$ was at 436 nm with the highest intensity. As the solvent polarity increases, the fluorescence emission peaks intensity gradually decreases in the order of $CHCl_3$, THF, DCM, DMF, MeOH, $CH_3CN$ and DMSO (Fig. 4d). It is noticed that in strong polar solvent DMSO, the emission peaks are observed at 414 nm and 439 nm with insignificant intensity. The Boc-L-Phe-TCF-1 in DMSO was observed to have an intensity decrease to ~96% of that in $CHCl_3$. The Fig. 4e shows the fluorescence emisison spectra of Boc-L-Tyr-TCF-1 in different solvents. In less polar $CHCl_3$ solvent, Boc-L-Tyr-TCF-1 displayed significant intense emisison peaks at 413 nm and 435 nm. The fluorescence emission peak shows decrease in intensity in the trend of $CHCl_3$, THF, DCM, DMF, MeOH, $CH_3CN$ and DMSO (Fig. 4e, Table 1). Boc-L-Tyr-TCF-1 exhibit less intense peaks at 414 nm and 437 nm on going from $CHCl_3$ to DMSO. The lowest intense peaks for the Boc-L-Tyr-TCF-1 in DMSO displayed with decrease to ~92% of that in $CHCl_3$. Similar trend was observed for Boc-L-Trp-TCF-1 fluorophore going from less polar $CHCl_3$ (peaks at 412 nm, 436 nm with significant intensity) to strong polar DMSO (peaks at 414 nm, 436 nm, with less

intensity) (Fig. 4f). As the solvent polarity enhances, the general trend in fluorescence spectra displayed decrease in peak intensity n the order of $CHCl_3$, THF, DCM, DMF, MeOH, $CH_3CN$ and DMSO (Fig. 4f, Table 1). The emission intensity of Boc-L-Trp-TCF-1 in $CHCl_3$ is very high, and ~92% decreased in DMSO. It has been observed that the emission intensity of Boc-L-Phe-TCF-1, Boc-L-Tyr-TCF-1 and Boc-L-Trp-TCF-1 is solvent dependent. In all three cases, the highest fluorescence emission intensity values are found in chloroform for Boc-L-Phe-TCF-1, Boc-L-Tyr-TCF-1 and Boc-L-Trp-TCF-1 and gradually decreases as the solvent polarity increases in the order of $CHCl_3$, THF, DCM, DMF, MeOH, $CH_3CN$ and DMSO. The decrease in fluorescence of Boc-L-Phe-TCF-1, Boc-L-Tyr-TCF-1 and Boc-L-Trp-TCF-1 in polar solvent could be attributed to the solvatochromism effect[21]. In addition, in polar solvent these Boc-L-Phe-TCF-1, Boc-L-Tyr-TCF-1 and Boc-L-Trp-TCF-1 fluorophores displayed low fluorescence emission intensity, which could be ascribed to the smaller energy difference between ground state and intramolecular charge transfer (ICT) state resulting into the selection of nonradiative pathway. In connection to this, the non-emissive state could be the result of effective state charge separation of the fluorophores in polar solvent[22]. The detailed solvatochromic analysis of Boc-L-Phe-TCF-1, Boc-L-Tyr-TCF-1 and Boc-L-Trp-TCF-1 was not carried out since the process is highly complex in nature and involves various interactions *e.g.* solubility, dynamic process, solvent-induced structural alteration, polarization effects, solute-solvent hydrogen bonding non-covalent interactions and aggregation of the fluorophores[23]. The UV-Vis and fluorescence spectral properties of Boc-L-Phe-TCF-1, Boc-L-Tyr-TCF-1 and Boc-L-Trp-TCF-1 were not studied in water at different *p*H due to their solubility issue.

We also investigated the *p*H responsiveness of L-Phe-TCF-1, L-Tyr-TCF-1 and L-Trp-TCF-1 in aqueous solution. The UV-Vis and fluorescence measurements in aqueous solution of *p*H 3, 5, 7, 9, and 11 were performed and displayed in Fig. 5 and the values were summarized in Table 2. The absorption spectra of L-Phe-TCF-1 (Fig. 5a) at *p*H 3 displayed strong peak at 400 nm ($\varepsilon = 1.04 \times 10^4\ M^{-1}\ cm^{-1}$) with shoulder peak at 333 nm ($\varepsilon = 0.71 \times 10^4\ M^{-1}\ cm^{-1}$) and 554 nm ($\varepsilon = 0.34 \times 10^4\ M^{-1}\ cm^{-1}$). At *p*H value 5, the absorption peaks at 333 nm ($\varepsilon = 0.57 \times 10^4\ M^{-1}\ cm^{-1}$) and 481 nm (broad) ($\varepsilon = 0.83 \times 10^4\ M^{-1}\ cm^{-1}$) were observed. Similarly, at *p*H 7, the absorption peaks were found at 336 nm ($\varepsilon = 0.63 \times 10^4\ M^{-1}\ cm^{-1}$) and 483 nm (broad) ($\varepsilon = 0.91 \times 10^4\ M^{-1}\ cm^{-1}$). The peaks were appeared at 336 nm ($\varepsilon = 0.91 \times 10^4\ M^{-1}\ cm^{-1}$) and broad peak 455 nm ($\varepsilon = 1.43 \times 10^4\ M^{-1}\ cm^{-1}$) at *p*H 9. When *p*H was changed to 11, the L-Phe-TCF-1 displayed absorption peaks at 336 nm ($\varepsilon = 1.24 \times 10^4\ M^{-1}\ cm^{-1}$) and broad peak at 481 m ($\varepsilon = 1.06 \times 10^4\ M^{-1}\ cm^{-1}$). The absorption peak at *p*H 3 found at 400 nm diminishes and the spectrum again displays new peaks with significant bathochromic shifts of 81 nm, 83 nm, 55 nm and 81 nm for the L-Phe-TCF-1 solutions at *p*H 5, 7, 9 and 11, respectively. Herein, the protonation and deprotonation state of $–NH_2$ in L-Phe-TCF-1 behaves differently as we move from acidic *p*H 3 to 5 to neutral 7 to basic 9 and *p*H 11, which in turn could be attributed to the changes in electronic donor/acceptor properties of $–NH_2$ functional group of L-Phe-TCF-1. In addition, we presume that L-Phe-TCF-1 displayed strong electrostatic interaction in acidic media. Similarly, the absorption properties of the L-Tyr-TCF-1 was examined at varying *p*H values of 3, 5, 7, 9 and 11 and depicted in Fig. 5b and summarized in Table 2. When the *p*H was 3, the two intense absorption peaks appeared at 399 nm ($\varepsilon = 1.75 \times 10^4\ M^{-1}\ cm^{-1}$) and 538 nm ($\varepsilon = 0.81 \times 10^4\ M^{-1}\ cm^{-1}$). At *p*H 5, the peaks appeared at 334 nm ($\varepsilon = 0.56 \times 10^4\ M^{-1}\ cm^{-1}$) and broad peak at 518 nm ($\varepsilon = 2.17 \times 10^4\ M^{-1}\ cm^{-1}$). The two peaks were observed at 336 nm ($\varepsilon = 0.66 \times 10^4\ M^{-1}\ cm^{-1}$) and 517 nm (broad peak) ($\varepsilon = 2.35 \times 10^4\ M^{-1}\ cm^{-1}$) at *p*H 7. At *p*H 9, the absorption peaks were found at 337 nm ($\varepsilon = 0.88 \times 10^4\ M^{-1}\ cm^{-1}$) and 516 nm (broad peak) ($\varepsilon = 2.52 \times 10^4\ M^{-1}\ cm^{-1}$). At higher *p*H of about 11, the L-Tyr-TCF-1 displayed two peaks at 336 nm ($\varepsilon = 1.16 \times 10^4\ M^{-1}\ cm^{-1}$) and 516 nm (broad peak) ($\varepsilon = 2.20 \times 10^4\ M^{-1}\ cm^{-1}$). As we change the *p*H values from acidic 3 to 5 and then to neutral 7 and further to basic 9 and 11, we observed the strong bathochromic shifts of 119, 118, 117 and 120 nm. These large red shifts compared to the absorption peak at 399 nm of L-Tyr-TCF-1 at *p*H 3, could be ascribed to the alteration in electronic donor/acceptor properties of $–NH_2$ present within the molecular skeleton. These results of the L-Tyr-TCF-1 at neutral as well as basic media implies that the presence of weaker electrostatic interaction within the $–NH_2$ group. In aqueous medium, the L-Trp-TCF-1 displayed characteristic UV-Vis absorbance bands within the 300 to 600 nm

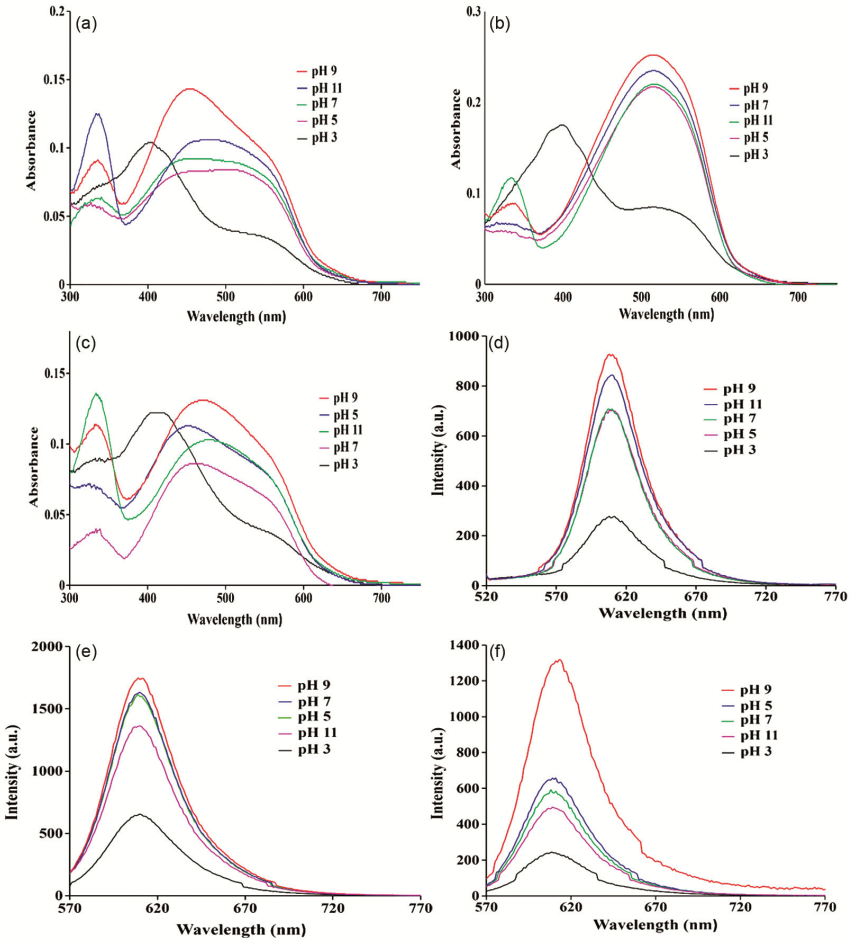


Fig. 5 — UV-Vis spectra of (a) L-Phe-TCF-1, (b) L-Tyr-TCF-1 and (c) L-Trp-TCF-1 and fluorescence emission spectra of (d) L-Phe-TCF-1, (e) L-Tyr-TCF-1 and (f) L-Trp-TCF-1 at different *p*H ranging from 3 to 11

Table 2 — UV-Vis absorption and fluorescence emission spectra of L-Phe-TCF-1, L-Tyr-TCF-1 and L-Trp-TCF-1 at different *p*H in aqueous media

| Spectroscopic Methods | *p*H values | L-Phe-TCF-1 | | L-Tyr-TCF-1 | | L-Trp-TCF-1 | |
|---|---|---|---|---|---|---|---|
| UV-Vis absorption spectra (nm) (Extinction coefficient ε ($M^{-1}$ $cm^{-1}$) | 3 | 400 (10400) & Shoulder peak at 333 (7100) | 554 (3400) | 399 (17500) | Broad peak 538 (8100) | 332 (8900) & 413 (12200) | Broad peak 564 (3500) |
| | 5 | 333 (5700) | Broad peak 481 (8300) | 334 (5600) | Broad peak 518 (21700) | 331 (7100) | Broad peak 451 (11300) |
| | 7 | 336 (6300) | Broad peak 483 (9100) | 336 (6600) | Broad peak 517 (23500) | 337 (3900) | Broad peak 460 (8600) |
| | 9 | 336 (9100) | Broad peak 455 (14300) | 337 (8800) | Broad peak 516 (25200) | 334 (11400) | Broad peak 470 (13100) |
| | 11 | 336 (12400) | Broad peak 481 (10600) | 336 (11600) | Broad peak 519 (22000) | 336 (13500) | Broad peak 472 (10200) |
| Fluorescence Emisison Spectra (nm) Excitation wavelength | 3 | 610 ($\lambda_{ex}$ = 510 nm) | | 610 ($\lambda_{ex}$ = 510 nm) | | 610 ($\lambda_{ex}$ = 550 nm) | |
| | 5 | 610 ($\lambda_{ex}$ = 510 nm) | | 610 ($\lambda_{ex}$ = 510 nm) | | 610 ($\lambda_{ex}$ = 550 nm) | |
| | 7 | 610 ($\lambda_{ex}$ = 510 nm) | | 610 ($\lambda_{ex}$ = 510 nm) | | 610 ($\lambda_{ex}$ = 550 nm) | |
| | 9 | 610 ($\lambda_{ex}$ = 510 nm) | | 610 ($\lambda_{ex}$ = 510 nm) | | 610 ($\lambda_{ex}$ = 550 nm) | |
| | 11 | 610 ($\lambda_{ex}$ = 510 nm) | | 610 ($\lambda_{ex}$ = 510 nm) | | 610 ($\lambda_{ex}$ = 550 nm) | |

wavelength range at *p*H = 3 to 11 (Fig. 5c). For lower *p*H value *e.g*. at 3, we observed an absorption peaks at 332 nm ($\varepsilon = 0.89 \times 10^4\ M^{-1}\ cm^{-1}$)., 413 nm ($\varepsilon = 1.22 \times 10^4\ M^{-1}\ cm^{-1}$) and 564 nm ($\varepsilon = 0.35 \times 10^4\ M^{-1}\ cm^{-1}$). Beyond *p*H 5 the absorption peak around 413 nm diminishes and new peaks were appeared. For *p*H 5, the absorption peaks appeared at 331 nm ($\varepsilon = 0.71 \times 10^4\ M^{-1}\ cm^{-1}$)., 451 nm ($\varepsilon = 1.13 \times 10^4\ M^{-1}\ cm^{-1}$). When the *p*H was further increased to 7, the UV-vis absorption bands appeared at 337 nm ($\varepsilon = 0.39 \times 10^4\ M^{-1}\ cm^{-1}$)., 460 nm ($\varepsilon = 0.86 \times 10^4\ M^{-1}\ cm^{-1}$). The more intense peaks were found at 334 nm ($\varepsilon = 1.14 \times 10^4\ M^{-1}\ cm^{-1}$)., 470 nm ($\varepsilon = 1.31 \times 10^4\ M^{-1}\ cm^{-1}$) at *p*H 9 solution of L-Trp-TCF-1 in water. At higher *p*H 11, the absorption peaks were observed at 336 nm ($\varepsilon = 1.35 \times 10^4\ M^{-1}\ cm^{-1}$)., 472 nm ($\varepsilon = 1.02 \times 10^4\ M^{-1}\ cm^{-1}$).

Thus, the increase in *p*H of the L-Trp-TCF-1 solution in water showed significant red-shifts of 38, 47, 57 and 59, when *p*H was changed to 5, 7, 9 and 11, respectively (Fig. 5c, Table 2). From this we conclude that the absorption spectra of the L-Trp-TCF-1 chromophore directly depends on the protonated and deprotonated form in an aqueous solution. This could be attributed to the strong electrostatic interaction at lower *p*H 3, whereas, at higher *i.e*. neutral and basic *p*H the L-Trp-TCF-1 exhibits wreaker indication within the $–NH_2$ base.

Furthermore, at different *p*H ranging from 3 to 11, we studied the fluorescence emission spectra of L-Phe-TCF-1, L-Tyr-TCF-1 and L-Trp-TCF-1 and displayed in Fig. 5d, Fig. 5e and Fig. 5f, respectively. Fig. 5d, showing the relative fluorescence of L-Phe-TCF-1 aqueous solution at *p*H 3, 5, 7, 9 and 11 has been recorded at 610 nm upon excitation at 510 nm. The fluorescence emission peaks appeared at 610 nm for *p*H 3, 5, 7, 9 and 11. The order of the fluorescence intensity of L-Phe-TCF-1 was as follows: *p*H 9 > *p*H 11 > *p*H 7 ≈ *p*H 5 > *p*H 3. There were no obvious fluorescence changes of L-Phe-TCF-1 observed at different *p*H conditions over the range of *p*H 3-11. At *p*H 3, the fluorescence intensity of L-Phe-TCF-1 is significantly lower, approximately ~70% decreased compared to *p*H 9. This further increases at *p*H 5 and remains constant at *p*H 7, ~24% lower compared to *p*H 9, reaches a maximum at *p*H 9, and then decreases slightly, ~9% at *p*H 11, as shown in Fig. 5d. Thus, the fluorescent amino acid L-Phe-TCF-1 probe displayed a highly sensitive response to *p*H. L-Phe-TCF-1 exhibits very low fluorescence in acidic conditions at *p*H 3, while the polyamine decorated 1,3,5-tristyrylbenzenes chromophore reported in the literature was highly fluorescent in acidic conditions[24]. This could be attributed to the reduction in fluorescence quenching due to the electrostatic repulsion between positively charged functional group within the molecular structure. The protonation of polyamine in acidic condition could prohibit the photoinduced electron transfer (PET). The significant increase in fluorescence intensity of L-Phe-TCF-1 as the change in *p*H from acidic condition of 3 to basic conditions of 9 and 11. This unobvious *p*H dependent behaviour of the L-Phe-TCF-1 chromophore could be attributed to our hypothesis that protonated $-NH_2$ functional group of phenylalanine could function as electron acceptors to quench the fluorescence of TCF subunit (Fig. 5d). This suggests that the fluorescence intensity of L-Phe-TCF-1 can be utilized to detect the *p*H of the cellular compartments within the live cells[25]. Further, we examined the fluorescence properties of the L-Tyr-TCF-1 in water at various *p*H 3, 5, 7, 9 and 11 up on excitation at 510 nm (Fig. 5e). It was found that fluorescent L-Tyr-TCF-1 is highly sensitive towards different *p*H conditions with varying the peak intensity (Fig. 5e). At *p*H 3, 5, 7, 9 and 11, the L-Tyr-TCF-1 exhibits fluorescent peak at 610 nm ($\lambda_{ex}$ = 510 nm). The order of fluorescence intensity was observed as *p*H 9 > *p*H 7 ≈ *p*H 5 > *p*H 11 > *p*H 3. It is surprizing that at higher acidic conditions particularly at *p*H 3, the fluorescent L-Tyr-TCF-1 probe displayed very low fluorescence intensity decreased by ~62% compared with *p*H 9. Whereas, with the increase in *p*H from 3 to 9, exhibits enhanced fluorescence, indicating the protonated $-NH_2$ functional group of tyrosine acts as acceptor, whereas the TCF-1 acts as donor moiety. It is surprising that, when we moved from *p*H 9 to *p*H 11, the fluorescence intensity was found to be slightly ~21% decreased, suggesting the $-NH_2$ group of tyrosine displayed slightly donor properties and TCF-1 acts as acceptor. This could be ascribed to the photoinduced electron transfer (PET) from primary amine of the tyrosine to the acceptor subunit TCF within the L-Tyr-TCF-1 molecular skeleton[26,27]. Similarly, as demonstrated in Fig. 5f, L-Trp-TCF-1 displayed the different fluorescence behaviour as *p*H changes from 3 to 11. It was found that as *p*H changes the fluorescence emission peak intensity alters in the order of *p*H 9 > *p*H 5 > *p*H 7 > *p*H 11 > *p*H 3. The change in the *p*H from acidic 3 to basic 9 showed

significant increases in fluorescence emission, indicating the protonated -$NH_2$ of tryptophan displayed donor behaviour, whereas the TCF acts as acceptor to quench the fluorescence of the L-Trp-TCF-1 *via* d-PET mechanism[28].

This investigation provides new path of the *p*H responsive aromatic amino acid functionalized (*E*)-2-(4-(4-aminostyryl)-3-cyano-5,5-dimethylfuran-2(5*H*)-ylidene) malononitrile (TCF-1) chromophore design with excellent absorbance and fluorescence properties.

## Conclusions

In summary, the UV-Vis absorption and fluorescence spectral properties of Boc-L-Phe-TCF-1, Boc-L-Tyr-TCF-1 and Boc-L-Trp-TCF-1 were established in different organic solvents. The absorbance and emisison properties of these chromophores are found to be solvent dependent. In addition, the UV-Vis absorption, and fluorescence intensity with different *p*H ranging from 3 to 11 of three amino acid derivatives L-Phe-TCF-1, L-Tyr-TCF-1 and L-Trp-TCF-1 has been investigated. The *p*H dependent UV-Vis changes of L-Phe-TCF-1, L-Tyr-TCF-1 and L-Trp-TCF-1 was mainly ascribed to the electrostatic interaction based aggregation of these chromophores. The *p*H dependent fluorescence intensity changes were demonstrated systematically, indicating surprising behaviour of the molecule at acidic as well as basic *p*H. The unprecedented fluorescence behaviour of the-Phe-TCF-1, L-Tyr-TCF-1 and L-Trp-TCF-1 bearing free amine (-$NH_2$) functional group in their deprotonated form at acidic and basic *p*H are interesting properties for possible bioimaging applications[29,30].

## Supplementary Information

Supplementary information is available in the website https://nopr.niscpr.res.in/handle/123456789/58776.

## Acknowledgements

Sidhanath Vishwanath Bhosale (IICT) is grateful for financial support from the Director, CSIR-IICT (MS No. IICT/Pubs./2025/415). D.D.U would like to thank CSIR, New Delhi for SRF fellowship. Sheshanath V. Bhosale (CUK) acknowledges University Grant Commission (UGC) Faculty Research Program, New Delhi, India (F.4-5(50-FRP) (IV-Cycle)/2017 (BSR)) for an award of Professorship.

## References

1 Alberts B, Johnson A, Lewis J, Raff M, Roberts K & Walter P, *Molecular Biology of the Cell. 4th ed*, (Garland Science, New York), 2002.

2 (a) Chan J, Dodani S C & Chang C, *J Nat Chem*, 4 (2012) 973; (b) Lavis L D & Raines R T, *Acc Chem Res*, 50 (2017) 375.

3 (a) Giepmans B N G, Stephen R A, Ellisman M H & Tsien R Y, *Science*, 312 (2006) 217; (b) Gao J, Strässler C, Tahmassebi D & Kool E, *J Am Chem Soc*, 124 (2002) 11590; (c) Mayer A & Neuenhofer S, *Angew Chem Int Ed Eng*, 33 (1994) 1044; (d) Hangauer M J & Bertozzi C R, *Angew Chem Inter Ed*, 47 (2008) 2394; (e) Reetz M T, *Angew Chem Int Ed*, 40 (2001) 284.

4 Cooper GM, *The Cell: A Molecular Approach*, *2nd ed*, (Sinauer Associates Inc, U S), 2000.

5 Fletcher S & Hamilton A D, *Curr Top Med Chem*, 7 (2007) 922.

6 (a) Ciruela F, *Curr Opin Biotechnol*, 19 (2008) 338; (b) Förster T, *Annalen der Physik*, 2 (1948) 55, (c) Cardullo R A, *Methods Cell Biol*, 81 (2007) 479; (d) Pfleger K D & Eidne K A, *Nat Meth*, 3 (2006) 165.

7 (a) Shimomura O, Johnson F H & Saiga Y, *J Cell Comp Physiol* 59 (1962) 223; (b) Tsien R Y, *Annu Rev Biochem*, 67 (1998) 509; (c) Heim R, Cubitt A B & Tsien R Y, *Nature*, 373 (1995) 663; (d) Day R N & Davidson M W, *Chem Soc Rev*, 38 (2009) 2887; (e) Chudakov D M, Matz M V, Lukyanov S & Lukyanov K A, *Physiol Rev*, 90 (2010) 1103.

8 Sinkeldam R W, Greco N J & Tor Y, *Chem Rev*, 110 (2010) 2579.

9 Teale F W & Weber G, *Biochem J*, 65 (1957) 476.

10 (a) Lavis L D & Raines R T, *ACS Chem Biol*, 9 (2014) 855; (b) Lavis L D & Raines R T, *ACS Chem Biol*, 3 (2008) 142; (c) Jun J V, Chenoweth D M & Petersson E J, *Org Biomol Chem*, 18 (2020) 5747.

11 Krueger A T & Imperiali B, *ChemBioChem*, 14 (2013) 788.

12 (a) Merkel L, Hoesl M G, Albrecht M, Schmidt A & Budisa N, *ChemBioChem* 11 (2010) 305; (b) Cheng Z, Kuru E, Sachdeva A & Vendrell M, *Nat Rev Chem*, 4 (2020) 275.

13 He M, Leslie T M & Sinicropi J A, C*hem Mat*, 14 (2002) 2393.

14 Tsuneda T, Quantum Chemistry. In: Density Functional Theory in Quantum Chemistry. Springer, Tokyo. (2014). https://doi.org/10.1007/978-4-431-54825-6_1.

15 *Gaussian 16*, *Revision B.01*, Frisch M J, Trucks G W, Schlegel H B, Scuseria G E, Robb M A, Cheeseman J R, Scalmani G, Barone V, Petersson G A, Nakatsuji H, Li X, Caricato M, Marenich A V, Bloino J, Janesko B G, Gomperts R, Mennucci B, Hratchian H P, Ortiz J V, Izmaylov A F, Sonnenberg J L, Williams-Young D, Ding F, Lipparini F, Egidi F, Goings J, Peng B, Petrone A, Henderson T, Ranasinghe D, Zakrzewski V G, Gao J, Rega N, Zheng G, Liang W, Hada M, Ehara M, Toyota K, Fukuda R, Hasegawa J, Ishida M, Nakajima T, Honda Y, Kitao O, Nakai H, Vreven T, Throssell K, Montgomery J A, Peralta Jr J E, Ogliaro F, Bearpark M J, Heyd J J, Brothers E N, Kudin K N, Staroverov V N, Keith T A, Kobayashi R, Normand J, Raghavachari K, Rendell A P, Burant J C, Iyengar S S, Tomasi J, Cossi M, Millam J M, Klene M, Adamo C, Cammi R, Ochterski J W, Martin R L, Morokuma K, Farkas

O, Foresman J B & Fox D J, *GaussView 5.0. Wallingford, E.U.A.*, (Gaussian, Inc., Wallingford CT), 2016.
16 O'Boyle N M, Tenderholt A L & Langner K M, *J Comp Chem*, 29 (2008) 839.
17 Sabeka H A Z, Alazalya A M M, Salahb D, Abdel-Samad H S, Ismail M A & Abdel-Shafi A A, *RSC Adv*, 10 (2020) 43459.
18 Georg H C, Coutinho K & Canuto S, *J Chem Phys*, 126 (2007) 034507.
19 Yoosefian M & Etminan N, *RSC Adv*, 6 (2016) 64818.
20 (a) Liu L, Sun Y, Wei S, Hu X, Zhao Y, Fan J, *Spectrochim Acta A Mol Biomol Spect*, 86 (2012) 120; (b) Turro N J, Ramamurthy V & Scaiano J C, *Principle of Molecular Photochemistry: An Introduction*, (University Science Books), 2009; (c) Nakahama T, Kitagawa D, Sotome H & Ito S, Miyasaka H & Kobatake S, *Photochem Photobiol Sci*, 15 (2016) 1254.
21 Chen F, Zhang W, Tian T, Bai B, Wang H & Li M, *J Phys Chem A*, 121 (2017) 8399.
22 Kawski A & Bojarski P, *Spectrochim Acta Part A*, 82 (2011) 527.
23 Marini A, Munoz-Losa A, Biancardi A & Mennucci B, *J Phys Chem B*, 114 (2010) 17128.
24 Pacheco-Liñán P J, Garzón A, Tolosa J, Bravo I, Canales-Vázquez J, Rodríguez-López J, Albaladejo J & García-Martínez J C, *J Phys Chem C*, 120 (2016) 18771.
25 Li S-A, Meng X-Y, Zhang Y-J, Chen C-L, Jiao Y-X, Zhu Y-Q, Liu P-P & Sun W, *Front Pharm*, 14 (2024) 1339518.
26 Jockusch S, Ramirez J, Sanghvi K, Nociti R, Turro N J & Tomalia D A, *Macromolecules*, 32 (1999) 4419.
27 Baker L A & Crooks R M, *Macromolecules*, 33 (2000) 9034.
28 Zhang J, Yang M, Mazi W, Adhikari K, Fang M, Xie F, Valenzano L, Tiwari A, Luo F-T & Liu H, *ACS Sens*, 1 (2016) 158.
29 Berezin M Y & Achilefu S, *Chem Rev*, 110 (2010) 2641.
30 Kobayashi H, Ogawa M, Alford R, Choyke P L & Urano Y, *Chem Rev*, 110 (2010) 2620.